

1 **Impacts of anemometer changes, site relocations and processing methods on**
2 **wind speed trends in China**

3 Yi Liu¹, Lihong Zhou¹, Yingzuo Qin¹, Cesar Azorin-Molina², Cheng Shen³,
4 Rongrong Xu^{1*}, Zhenzhong Zeng^{1*}

5 ¹ School of Environmental Science and Engineering, Southern University of Science
6 and Technology, Shenzhen, China

7 ² Centro de Investigaciones sobre Desertificación, Consejo Superior de
8 Investigaciones Científicas (CIDE, CSIC-UV-Generalitat Valenciana), Climate,
9 Atmosphere and Ocean Laboratory (Climatoc-Lab), Moncada, Valencia, Spain

10 ³ Regional Climate Group, Department of Earth Sciences, University of Gothenburg,
11 Gothenburg, Sweden

12
13 * Correspondence: xurr@sustech.edu.cn (R. Xu); zengzz@sustech.edu.cn (Z. Zeng)

14 Manuscript for *Atmospheric Measurement Techniques*

15 December 22, 2023

16

17 **Abstract**

18 *In-situ* surface wind observation is a critical meteorological data source for various
19 research fields. However, data quality is affected by factors such as surface friction
20 changes, station relocations, and anemometer updates. Previous methods to address
21 discontinuities have been insufficient, and processing methods have not always
22 adhered to World Meteorological Organization (WMO) World Climate Programme
23 guidelines. We analyzed data discontinuity caused by anemometer changes and
24 station relocations in China's daily *in-situ* near-surface (~ 10m) wind speed
25 observations and the impact of the processing methods on wind speed trends. By
26 comparing the wind speed discontinuities with the recorded location changes, we
27 identified 90 stations that showed abnormally increasing wind speeds due to
28 relocation. After removing those stations, we followed a standard quality control
29 method recommended by the World Meteorological Organization to improve the data
30 reliability and applied Thiessen Polygons to calculate the area-weighted average wind
31 speed. The result shows that China's recent reversal of wind speed was reduced by
32 41% after removing the problematic stations, with an increasing trend of 0.017 m s^{-1}
33 year^{-1} ($R^2 = 0.64$, $P < 0.05$), emphasizing the importance of robust quality control and
34 homogenization protocols in wind trend assessments.

35 **Keywords.** wind speed trends; anemometer changes; station relocations; processing
36 methods; quality control; data homogenization

37

38 **1. Introduction**

39 *In-situ* surface wind observation is a key meteorological data that has been used in
40 various avenues of research, e.g., wind power evaluation (Tian et al., 2019; Zeng et
41 al., 2019; Liu et al. 2022a), extreme wind hazard monitoring and prevention (Liu et
42 al., 2022b), and evapotranspiration analysis (Rayner, 2007; McVicar et al., 2012), to
43 name but a few. The application of robust quality control and homogenization
44 protocols are crucial for generating reliable wind speed time series for further trend
45 and variability analyses (Azorin-Molina et al., 2014; Azorin-Molina et al., 2019).

46 Wind data quality is affected by surrounding surface friction change, station
47 location issues, and anemometer changes in type and height (Masters et al., 2010;
48 Wan et al., 2010; Cao & Yan, 2012; Hong et al., 2014; He et al., 2014; Azorin-Molina
49 et al., 2018; Camuffo et al., 2020). Surrounding surface friction changes are mainly
50 associated with urbanization (Zhang et al., 2022) and vegetation growth (Vautard et
51 al., 2010), which modify wind speed fields around the stations. Because of these
52 issues, stations are relocated to satisfy observing criteria (Trewin, 2010). Station
53 relocation is quite common in rapidly developing countries. For instance, about 60%
54 of stations in China experienced relocation (Sohu, 2004). Some relocation-caused
55 breakpoints have been corrected by parallel observations (i.e. operating observations
56 for an overlapping period at both the old and new observing stations; CMA, 2011;
57 CMA, 2012; WMO, 2020), but not all (Feng et al., 2004; Fu et al., 2011; Tian et al.,
58 2019; Yang et al., 2021). Besides relocation caused by rapid urbanization (or
59 vegetation growth), updates to automatic anemographs at the beginning of the 21st
60 century in China also caused discontinuities in wind series (Fu et al., 2011).

61 Scientists have tried different methods to handle discontinuities. Tian et al. (2019)
62 and Yang et al. (2021) deleted stations with recorded changes in latitudes, longitudes
63 or altitudes, but they omitted to check whether those recorded relocations caused an
64 abrupt discontinuity in the time series or if parallel observations have corrected them.
65 This results in some stations being mistakenly deleted and significantly reduced the
66 number of available stations. Other research used statistical methods to detect or
67 correct the time series' abnormal breakpoint (Feng et al., 2004; Wang, 2008).

68 However, without examining the causes behind the discontinuity, this may also
69 mistakenly delete stations with natural abrupt climatic changes (Bathiany et al., 2003).
70 Combining those two methods by matching discontinuity with recorded station
71 relocation is needed. Li et al. (2018) have manually checked the station histories for
72 nine stations in North West China, but an algorithm is required to apply this approach
73 to large datasets.

74 Besides data discontinuities, the processing method also affects the wind series.
75 There are two critical steps in the processing: 1) selecting qualified stations and 2)
76 calculating the average value. As for the first step, World Meteorological
77 Organization (WMO) World Climate Programme suggests deleting stations with
78 either too much missing data or continuous missing data (WMO, 2017). Previous
79 studies only constrained the number of missing values monthly (Zeng et al., 2019),
80 yearly (Tian et al., 2019) or even in the whole period (Yang et al., 2021) but didn't
81 check whether the missing values were continuous. As for the second step, most
82 studies used the station average as the mean wind speed (Li et al., 2017; Zeng et al.,
83 2019; Tian et al., 2019; Yang et al., 2021; Shen et al., 2021; Zha et al., 2021).
84 However, given station distribution and wind speed spatial variation are often
85 inhomogeneous with larger wind but fewer station in Northwest while smaller wind
86 but more stations in Southeast (Feng et al., 2004; Fu et al., 2011; Liu et al., 2019), the
87 wind variation in Northwest is underrepresented because of few stations. An
88 improved average method (area weighted average) to rearrange the weight for each
89 station based on the area it represents is needed and Thiessen Polygon (Thiessen,
90 1991) is widely used in which the area is only determined by the station locations
91 while other method like grids is sensitive to the grids chosen.

92 Herein, taking stations in China as an example, we analyzed the existing data
93 discontinuities and their potential causes. Furthermore, we propose an improved
94 solution by using an algorithm to compare the statistic breakpoint with the recorded
95 relocation to double-check the discontinuity caused by relocation. Then using WMO's
96 quality control criteria and Thiessen Polygon (Thiessen, 1911), we generated wind

97 speed time series without temporal bias caused by heterogeneous missing values and
98 spatial biases caused by uneven station distribution.

99

100 **2. Dataset and methodology**

101 **2.1 WMO quality control method**

102 We used the China Surface Climatic Data Daily Data Set (CSD) (Version 3.0)
103 from the China Meteorological Data Service Center (<http://data.cma.cn/en/?r=data/>;
104 last accessed March 2020). The quality control method is recommended by WMO
105 (2017), which required the following criteria before using the daily mean values in a
106 month as monthly mean values: (1) <11 missing daily values in a month; (2) <5
107 consecutive missing daily values in a month; (3) Complete monthly values for every
108 month during the study period. The station excluded by each criterion can be found in
109 Table S1.

110

111 **2.2 Station location changes in record**

112 CSD provides daily wind speed and location information for 840 stations for
113 1961-2019. But there are some mistakes in the daily location records. For example, if
114 the station location changed from A to B and back to A within a month, B is
115 potentially a mistaken record. Therefore, we first use mode (the statistic term meaning
116 the value that appears most often, here referring to the location with the highest
117 frequency in a month) to resample the daily location to the monthly location. Second,
118 considering that recorded longitude and latitude has the same spatial resolution of
119 minutes, we defined the threshold of location change as the minimum accuracy of the
120 longitude and latitude record, i.e., one minute. That is 1.85 km for longitude and 1.85
121 $\text{km} \times \cos\phi$ for latitude, where ϕ is the latitude. Third, as for altitude, we allow a 20m
122 measuring error following Tian et al. (2019). A station with more than 20m change in
123 altitude will be considered as relocation. It is noteworthy that CSD labels uncertain
124 altitude records by adding 10 km to the raw data (CMA, 2017), which are considered
125 as no observations in our analysis. This way, we identified 432 stations as relocations

126 from the 601 qualified stations after applying the WMO quality control (details in
127 Table S2).

128

129 **2.3 Breakpoint detection and the comparison with recorded relocation**

130 We used Pruned Exact Linear Time (PELT) method (Killick, Fearnhead &
131 Eckley, 2012) to detect the jumps in the mean level in the monthly wind speed time
132 series (Fig 4a, Fig 4c). This method is a wrapped function named *findchangepts* in
133 Matlab. PELT is essentially a traversing method. For a time series with N values
134 $(x_1, x_2 \dots x_N)$, the function uses equations 1 & 2 to calculate the total residual errors
135 (J) for each point (k) assumed as a breakpoint. The point with the most significant
136 change in the mean (lowest total residual errors, J) is reported as the breakpoint. The
137 breakpoints here can be caused by artificial relocations or natural climate changes.

$$138 \quad J(k) = \sum_{i=1}^{k-1} (x_i - \text{mean}([x_1 \dots x_{k-1}]))^2 + \sum_{i=k}^N (x_i - \text{mean}([x_k \dots x_N]))^2 \quad (1)$$

$$139 \quad \text{mean}([x_m \dots x_n]) = \frac{1}{n-m+1} \sum_{r=m}^n x_r \quad (2)$$

140 Then we use relocation records to separate changes brought by artificial
141 relocation from changes in natural climate. If the breakpoint and one of the relocation
142 dates (some stations have more than one relocation record) happened in the same two
143 months, we will consider that the time series is significantly affected by the
144 relocation, and the station will be deleted. Stations with natural-climate-caused
145 location changes will be reserved.

146 The change point in the trend of the annual national average wind speed (Fig 2b,
147 Fig 5b) is detected following the method used by Wang et al. (2011). All the trends
148 reported are based on the least square fits.

149

150 **3. Results and discussion**

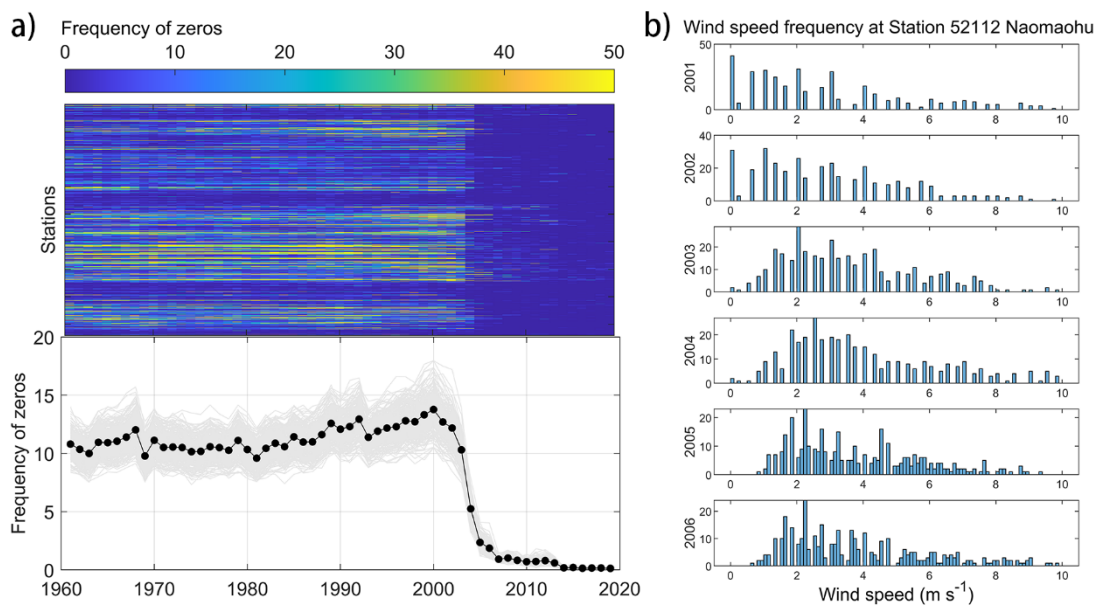
151 **3.1 Data issue due to anemometer changes**

152 We found a clear decline in the frequency of zeros (zero wind speed) in most
153 CSD stations between 2002 and 2007 (Figure 1a), from 10-14 days per year to less

154 than two days per year. This clear drop is not a result of wrongly taking zero values as
155 no observations (NaN) as happened in the Integrated Surface Dataset (ISD, Dunn et
156 al., 2022), as no abrupt increase in NaN frequency was observed (Supplementary
157 Figure S1). Instead, the decline is accompanied by a decrease in measure uncertainty:
158 i.e., the measurement intervals became narrow (from 0, 0.3, 0.5, 0.7, 0.8, 1.0 m s⁻¹,
159 etc. to 0, 0.1, 0.2, 0.3 m s⁻¹, etc.; Figure 1b and Supplementary Figure S2). Taking
160 Station Naomaohu in Xinjiang (station ID: 57432) as an example, from 2002 to 2003,
161 zero values decreased from more than 30 days per year to less than five days per year
162 and wind speed records changed from 0, 0.3, 0.7, 1.0 m s⁻¹, etc. to 0, 0.3, 0.5, 0.8, 1.0
163 m s⁻¹, etc. Since 2004, the measurement was further improved to 0.1, 0.2, 0.3... m s⁻¹
164 and zeros values almost disappeared (Figure 1b).

165 This change is potentially caused by the transformation in measure frequency,
166 anemometer type and data logging, based on the station history recorded by Xin et al.
167 (2012). As for measurement frequency, in 2003, Station Naomaohu changed from 3
168 observations per day (i.e., 8:00, 14:00 and 20:00, China Standard Time) to four times
169 per day (2:00, 8:00, 14:00 and 20:00, China Standard Time). The increase in the
170 frequency of measurements decreases zeros in daily wind data, as only if all
171 observations report zero wind speeds, will the daily data (i.e., the average of all
172 observations in a day; CMA, 2017) be recorded as zero. Then in 2005, the EL
173 (Electric Logging) contact anemograph (Xin et al., 2012, Zhang et al., 2020), which
174 required manual recording, was replaced by the EC (Electric Coding) photoelectric
175 encoder self-recording type (Xin et al., 2012). Both EL and EC types of anemographs
176 use cup anemometers to measure wind speed. However, the EL type measures the
177 times of electronic contact (e.g., 200 meters rotation distance per contact) in a time
178 period, resulting in discrete records, while the EC type uses the Grey Code encoder
179 rotating with the cup anemometers to obtain a more precise wind speed record. This
180 anemograph change further decreases the likelihood of recording zero daily wind
181 speed because the updated new anemometers are more sensitive, and even very low
182 wind speeds will be measured with a value instead of recorded as zero (Azorin-
183 Molina et al., 2018). The smooth increasing frequency of zero values from 1960 until

184 2000 also supports this statement (Figure 1a): the longer the anemometer is used, the
 185 less sensitive it will become, and hence a greater wind speed will be required to
 186 record a non-zero value (Azorin-Molina et al., 2018), overall increasing the zero
 187 values. As for the change in data accuracy, there are two reasons: 1) EL type
 188 anemograph only measures the times of electronic contact (200 meters rotation
 189 distance per contact) in 10 mins, therefore it has discrete records. For example, one
 190 contact means 0.3 m s^{-1} (200m/600s) and two contacts means 0.7 m s^{-1} (400m/600s)
 191 (Hu et al., 2009) while EC type has more accurate records using the Grey Code; 2) the
 192 data logging changed from manual reading, calculating and rounding to instrument
 193 automatically calculating and retaining one decimal place. This example shows us the
 194 importance of recording siting criteria, required functional specifications of wind
 195 sensors and maintenance policy. However, those records are missing for most of the
 196 stations which hindered the quality classification and data processing.



197
 198 **Figure 1. Changes in wind speed data caused by anemometer updates. a)**
 199 Decrease of frequency of zeros. Each horizontal bar in the upper figure represents one
 200 station and there are 840 stations in total. The color indicates the frequency of zeros
 201 (days per year). The black dotted line in the lower figure is the average annual
 202 frequency of zeros of all the stations. The 300 grey lines are sample averages, each
 203 containing 40% amount of the total stations. **b)** Frequency (days per year) of daily

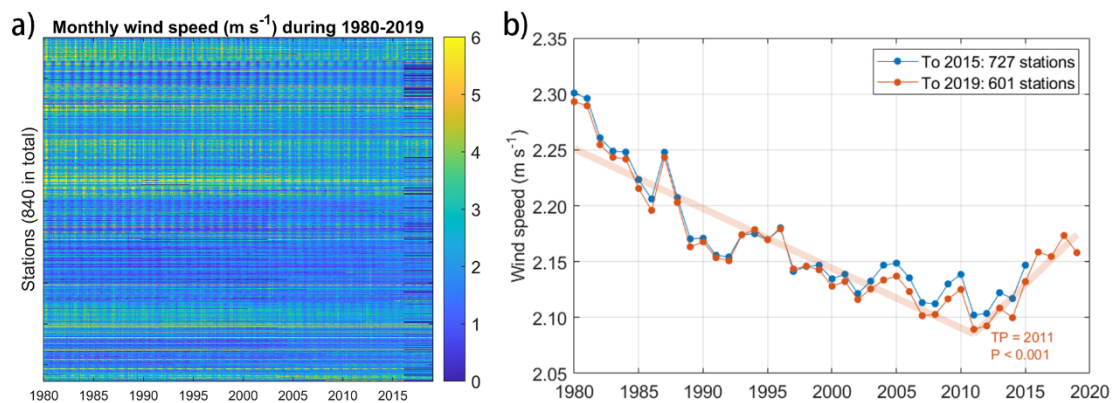
204 wind speed measurements between 2001 and 2006 for Station #52112 Naomaohu
205 (43°45'N, 94°59'E, 479.0 m a.s.l.)

206

207 3.2 Quality-controlled series

208 Following WMO's criteria, we generated the monthly average wind speed for
209 each station (Figure 2a). We found that since January 2016, there have been 126
210 stations that no longer have records (distribution see Figure S3). We compared the
211 time series with and without these stations and found the difference is not significant
212 (t-test $P < 0.001$, Figure 2b). To obtain a longer time series including recent years'
213 data, we deleted the 126 stations and only used the 601 stations with complete
214 monthly average wind speeds for 1980-2019. The breakpoint was detected in 2011 (P
215 < 0.001) with a decreasing trend of $-0.011 \text{ m s}^{-1} \text{ year}^{-1}$ ($R^2 = 0.84$, $P < 0.001$) before
216 the breakpoint and an increasing trend of $+0.022 \text{ m s}^{-1} \text{ year}^{-1}$ ($R^2 = 0.87$, $P < 0.001$)
217 after.

218



219

220 **Figure 2. Monthly average wind speed after being filtered by WMO's criteria. a)**

221 Each horizontal bar represents one station. Months with no data (NaNs) are

222 represented by the deepest blue. **b)** Comparison of the monthly average wind speed

223 for the short- (1980-2015; 727 stations) and long-period (1980-2019; 601 stations)

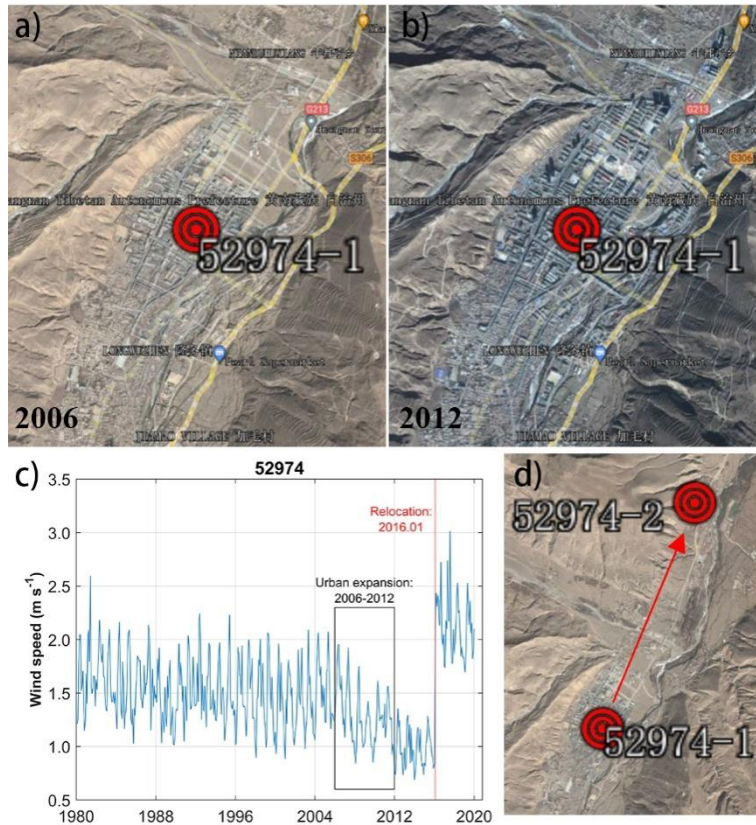
224

225 3.3 Station relocations caused by urbanization

226 Another key factor influencing wind speed measurements is the relocation of

227 stations. We found that there is a clear data jump caused by relocations in some of the

228 stations. Taking the station located in Qinghai (station ID 52974) as an example, we
229 detected an abrupt jump in wind speed in January 2016. This date coincides with the
230 relocation of the station from 35°31'N, 102°01'E (ID 52974-1) in December 2015 to
231 35°33'N, 102°02'E (ID 52974-2) in January 2016 (Figures 3c & 3d). The relocation is
232 potentially attributed to the urban growth around the station. As viewed by satellite
233 images from Google Earth Pro, there is a rapid urban expansion from 2006 (Figure
234 3a) to 2012 (Figure 3b), especially towards the Northeast of the station, during wind
235 speed records also experienced a decrease (Figure 3c). A similar decrease in both
236 daily mean wind speed and maximum wind speed caused by urbanization was also
237 reported in the Yangtze River region (Zhang et al., 2022). To eliminate the effect of
238 buildings on the wind speed measurements, Station 52974 was moved to 4 km away
239 from its previous location (Figure 3d) so that wind speed is properly measured
240 without artificial obstacles in the surroundings. However, this estimation of roughness
241 change based on satellite data is rough. A more proper way as required by the World
242 Climate Data and Monitoring Programme is to record the change in the station
243 logbook (WMO, 2018), which will provide more reliable information about the
244 quality of the data. But most stations don't have such a record. Despite the absence of
245 mete data, we used an established global roughness model through satellite albedo
246 observations to monitor alterations in surface roughness. For the selected station, we
247 employed the roughness estimation technique devised by Chappell & Webb (2016) to
248 analyze changes in roughness across a 5 km x 5 km area encompassing the station's
249 location. Our quantitative examination of roughness alterations aligns with the
250 findings derived from satellite imagery analysis, affirming a pronounced increase in
251 roughness between 2000 and 2010 (Supplementary Figure S4). This increase in
252 roughness likely contributed to the observed decline in wind speed and ultimately
253 compelled the relocation of the station.
254



255

256 **Figure 3. Example of station relocation caused by rapid urbanization growth. a-**

257 **b) Landsat images crop from Google Earth near Station 52974 in 2006 and 2012,**

258 **respectively. c) the wind speed change with urbanization and relocation. d) Landsat**

259 **images of the station relocation crop from Google Earth.**

260

261 Though some stations were influenced by station relocation as shown in Figure 3,

262 a larger fraction (79%) of stations show no change in wind speed after the relocation.

263 Further checking the raw record of locations for those stations, we find that one

264 reason is that some “relocations” result from wrong location records. For example,

265 Station 52974 is mistakenly detected with three relocations (Figure 4a). However,

266 only the first relocation is real and the latter two are results of location encoding

267 change from 10202 (interpreted as 102°02′) to 1022 (interpreted as 10°22′) and back.

268 Another possible reason is that the relocation did happen but the data has been

269 corrected. According to the *Provisional Regulations on Relocation, Construction and*

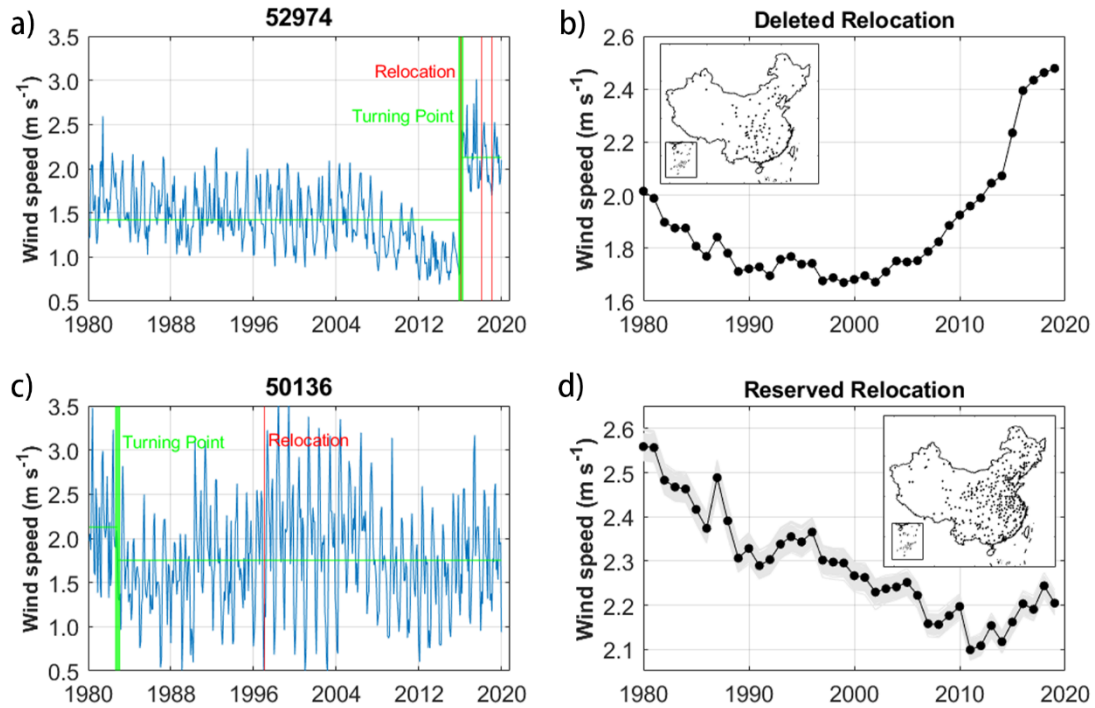
270 *Removal of National Ground Meteorological Observation* announced by China’s

271 government in 2012, station relocations should have 1-2 years of parallel observations

272 for data correction (CMA, 2012). This process may fix some of those discontinuities
273 but not all (Feng et al., 2004; Fu et al., 2011; Tian et al., 2019; Yang et al., 2021). For
274 example, Station 59287, the only national basic weather station in Guangzhou,
275 experienced two relocations in both 1996 and 2011, which is confirmed by the
276 metadata (CMA, 2011). After correction, the 1996 relocation doesn't show a sharp
277 breaking point but the 2011 one does (Supplementary Figure S5).

278 To examine whether the relocation caused a substantial change in the wind speed
279 record, we identified the most abrupt change in the wind speed time series and
280 checked whether a relocation happened near the change point (see details in *Methods*
281 2.3). Out of the 432 relocated stations, 90 were deleted because the most significant
282 shift in mean is at the time of the relocation, and hence this is the most likely cause.
283 We then took the average of the “deleted relocation” stations and “reserved
284 relocation” stations separately. The “deleted relocation” group shows an abnormally
285 rapid increase in the recent two decades (Figure 4b). While the “reserved relocation”
286 group is similar to stations without relocation (Supplementary Figure S6). To exclude
287 the impact of different station counts in each category (fewer stations mean higher
288 sensitivity to the individual abnormal station), we performed 300 samples using a
289 random draw of 90 stations from the “reserved relocation” group and showed them in
290 grey lines in Figure 4d. None of the grey lines shows an abnormal trend as the
291 “deleted relocation” group. This proves that our method is efficient in identifying
292 problematic stations.

293



294

295 **Figure 4. Comparison of deleted relocated stations and reserved ones. a)** The
 296 wind speed data breakpoint and relocations of one example of deleted relocation,
 297 Station 52974. **b)** The station average wind speed of 90 deleted relocated stations. The
 298 inset shows the station distribution across China. **c)** One example of reserved
 299 relocation, Station 50136. **d)** The station average wind speed of 342 reserved
 300 relocated stations. The grey lines are the averages of 300 samples, each with 90
 301 randomly drawn reserved relocated stations. Maps information are from Department
 302 of Natural Resources standard map service system of China.

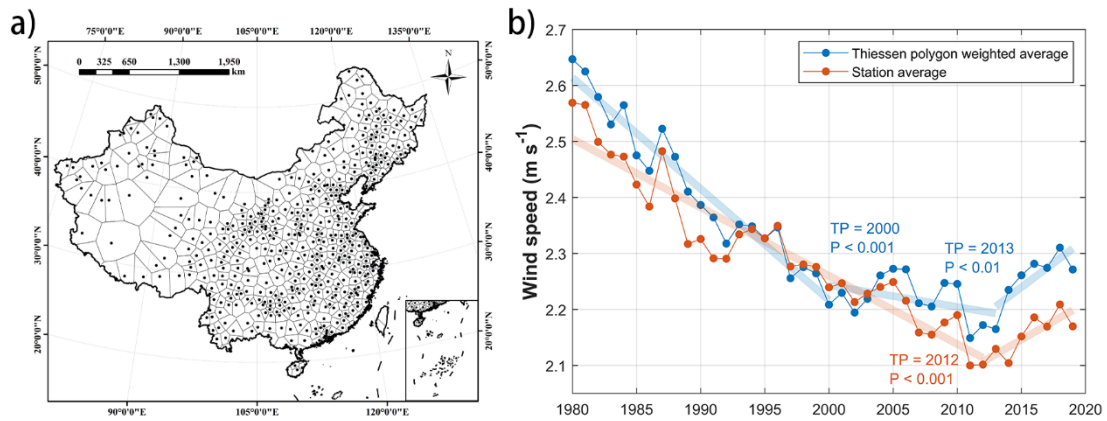
303

304 3.4 Average method used to calculate the national average

305 In the station average time series, the breakpoint was detected in 2012 ($P < 0.001$)
 306 with a trend of $-0.012 \text{ m s}^{-1} \text{ year}^{-1}$ ($R^2 = 0.90$, $P < 0.001$) before and $+0.013 \text{ m s}^{-1} \text{ year}^{-1}$
 307 ($R^2 = 0.70$, $P < 0.01$) after (Figure 5b). The increasing trend decreased by 41% after
 308 deleting those relocation-affected stations, compared with the $+0.022 \text{ m s}^{-1} \text{ year}^{-1}$ in
 309 Figure 2b (also reported by Liu et al., 2022a). But the trend is larger than the $+0.011$
 310 $\text{m s}^{-1} \text{ yr}^{-1}$, reported by Yang et al. (2021), with all the recorded location changed
 311 stations deleted without checking whether the station is affected by the relocation.

312 We further used Thiessen Polygon (Thiessen, 1911) to give different weights to
313 each station according to their representing area, i.e., large weight for stations located
314 in sparse stations area (Figure 5a) and compare the result with the station average
315 (Figure 5b). The Thiessen Polygon method, also known as the Voronoi Diagram, is a
316 spatial analysis technique often employed in hydrology and climatology. It involves
317 tessellating a region into polygons based on point data, such that each polygon
318 encompasses only one data point, and every location within a polygon is closer to its
319 associated point than any other. This method is particularly useful for interpolating
320 values across a region when the exact nature of change between points is unknown or
321 when changes are abrupt. By drawing perpendicular bisectors between adjacent data
322 points, the entire area is divided, with each polygon assuming the value of its
323 associated data point. While straightforward and clear in its delineation, the Thiessen
324 Polygon method assumes uniform variation within each polygon. The Thiessen
325 polygon weighted average is overall higher than the station average. This can be
326 explained by the increasing weight of stations in North West China with higher wind
327 speeds (Liu et al., 2019). While in the Thiessen polygon weighted average time series,
328 there are two breakpoints in 2000 ($P < 0.001$) and 2013 ($P < 0.01$). The trend changes
329 from quick decrease ($-0.020 \text{ m s}^{-1} \text{ year}^{-1}$, $R^2 = 0.94$, $P < 0.001$) to unstable moderate
330 decrease ($-0.004 \text{ m s}^{-1} \text{ year}^{-1}$, $R^2 = 0.17$, $P = 0.14$) and quickly increase ($+0.017 \text{ m s}^{-1}$
331 year^{-1} , $R^2 = 0.64$, $P < 0.05$). The increasing trend in the recent decade increased by
332 31% (from $+0.013 \text{ m s}^{-1} \text{ year}^{-1}$ to $+0.017 \text{ m s}^{-1} \text{ year}^{-1}$) after using the Thiessen
333 polygon approach. This is because the weights of stations in North West and South
334 West are increased when calculating the average and those area has strong increasing
335 wind speed trend (Figure S7). Despite the Thiessen polygon approach already
336 utilizing the nearest station observation to represent wind speed in locations lacking
337 direct observations, it remains unsatisfactory due to the intricate spatial variability of
338 wind speed attributed to complex terrains. To enhance the accuracy of wind speed
339 interpolation, a more comprehensive model necessitates additional observations
340 within areas characterized by complex terrain.

341



342

343 **Figure 5. Thiessen polygons and the comparison between Thiessen polygon**
 344 **weighted average and station average. a)** The Thiessen polygon map of the 511
 345 qualified stations. **b)** The comparison of station average wind speed (orange line) and
 346 Thiessen polygon weighted average (blue line) across China for 1980-2019. The
 347 linear fitting models are shown in translucent thick lines accordingly. Maps
 348 information are from Department of Natural Resources standard map service system
 349 of China.

350

351 4. Conclusions

352 Continuity is crucial for meteorological observation data. However, either the
 353 updates in the anemograph, the relocation caused by urbanization or the methods of
 354 data logging will affect wind speed data continuity. In this study, we comprehensively
 355 examined the discontinuity in wind speed data using a Chinese dataset. We found that
 356 updates to the automatic anemometer improved the observation frequency and
 357 instrument sensitivity, decreasing the zero-value daily wind speed data and increasing
 358 data accuracy. We also propose comparing the discontinuity in time series with
 359 recorded station relocation to check whether a relocation caused a breakpoint. We
 360 found that 90 stations were affected by the relocation and show a quickly increasing
 361 wind speed in the recent two decades. After excluding those problematic stations, the
 362 wind speed reversal trend is reduced by 41% but still strong ($P < 0.001$, with an
 363 increasing trend of $+0.013 \text{ m s}^{-1} \text{ year}^{-1}$). The increasing trend reaches $+0.017 \text{ m s}^{-1}$
 364 year^{-1} ($R^2 = 0.64$, $P < 0.05$) after using Thiessen Polygon, which gives the stations in

365 North West China a larger weight because their small number but located in a large
366 area.

367 Though lots of methods (Masters et al., 2010; Wan et al., 2010; Cao & Yan,
368 2012; Hong et al., 2014; He et al., 2014; Azorin-Molina et al., 2018; Camuffo et al.,
369 2020) were proposed to handle those problems, a comprehensive summary of them is
370 missing. Also, it is hard for external researchers to provide a better solution without a
371 collaboration with National Weather Services and the access to station data records
372 and/or metadata. Therefore, we hope National Weather Services could improve the
373 data quality based on these feedbacks and World Climate Data and Monitoring
374 Programme's guides, and complete the process by introducing an R package with
375 open-source code on GitHub and publishing the metadata. This way, not only the data
376 is easier to get and process, but also researchers can contribute to improve the dataset.
377 One such example is the "rnpn" package to access and process USA National
378 Phenology Network data (<https://github.com/usa-npn/rnpn>). Anyway, all raw data
379 processing has limitations and adds additional uncertainty. As we keep reporting
380 problems in datasets and improving our processing method, we should also pay more
381 attention to increasing the quality and homogeneity of the wind data. This requires
382 raising awareness of the importance of protecting the environment around the
383 observation station and avoiding relocations.

384

385 **Supplemental Information**

386 Document S1. Supplemental Information, Table S1, Figures S1 – S7.

387

388 **Acknowledgements**

389 Thank Robert Dunn (UK Met Office) for discussions and comments on the
390 manuscript. Thank Adrian Chappell for providing the surface roughness data. The
391 authors wish to acknowledge the reviewers for their detailed and helpful comments to
392 the original manuscript.

393

394 This study was supported by the National Natural Science Foundation of China (grant
395 no. 42071022), the Swedish Formas (2019–00509 and 2017–01408) and VR (2021–
396 02163 and 2019–03954), and the start-up fund provided by Southern University of
397 Science and Technology (no. 29/Y01296122). C. A-M. was supported by VENTS
398 (GVA-AICO/2021/023), the CSIC Interdisciplinary Thematic Platform (PTI) Clima
399 (PTI-CLIMA), the 2021 Leonardo Grant for Researchers and Cultural Creators,
400 BBVA Foundation, and the “Unidad Asociada CSIC-Universidad de Vigo: Grupo de
401 Física de la Atmosfera y del Océano”.

402

403 **Data availability statement**

404 The data that support the findings of this study are available upon request from the
405 authors.

406

407 **Author contributions**

408 **Zhenzhong Zeng:** Conceptualization, Methodology **Yi Liu:** Methodology, Software,
409 Writing – Draft **Lihong Zhou:** Methodology, Data Curation **All other authors:**
410 Writing – Review & Editing

411

412 **Declaration of interest**

413 The authors declare no competing financial interests.

414

415 **References.**

- 416 1. Azorin-Molina, C., Guijarro, J. A., McVicar, T. R., Trewin, B. C., Frost, A. J.,
417 and Chen, D.: An approach to homogenize daily peak wind gusts: An application
418 to the Australian series, *International Journal of Climatology*, 39, 2260–2277,
419 <https://doi.org/10.1002/joc.5949>, 2019.
- 420 2. Azorin-Molina, C., Vicente-Serrano, S. M., McVicar, T. R., Jerez, S., Sanchez-
421 Lorenzo, A., López-Moreno, J.-I., Revuelto, J., Trigo, R. M., Lopez-Bustins, J.
422 A., and Espírito-Santo, F.: Homogenization and Assessment of Observed Near-
423 Surface Wind Speed Trends over Spain and Portugal, 1961–2011, *Journal of*
424 *Climate*, 27, 3692–3712, <https://doi.org/10.1175/JCLI-D-13-00652.1>, 2014.
- 425 3. Azorin-Molina, C., Asin, J., McVicar, T. R., Minola, L., Lopez-Moreno, J. I.,
426 Vicente-Serrano, S. M., and Chen, D.: Evaluating anemometer drift: A statistical
427 approach to correct biases in wind speed measurement, *Atmospheric Research*,
428 203, 175–188, <https://doi.org/10.1016/j.atmosres.2017.12.010>, 2018.
- 429 4. Bathiany, S., Scheffer, M., van Nes, E. H., Williamson, M. S., and Lenton, T. M.:
430 Abrupt Climate Change in an Oscillating World, *Sci Rep*, 8, 5040,
431 <https://doi.org/10.1038/s41598-018-23377-4>, 2018.
- 432 5. Camuffo, D., della Valle, A., Becherini, F., and Zanini, V.: Three centuries of
433 daily precipitation in Padua, Italy, 1713–2018: history, relocations, gaps,
434 homogeneity and raw data, *Climatic Change*, 162, 923–942,
435 <https://doi.org/10.1007/s10584-020-02717-2>, 2020.
- 436 6. Cao, L. and Yan, Z.: Progress in Research on Homogenization of Climate Data,
437 *Advances in Climate Change Research*, 3, 59–67,
438 <https://doi.org/10.3724/SP.J.1248.2012.00059>, 2012.
- 439 7. Chappell, A. and Webb, N. P.: Using albedo to reform wind erosion modelling,
440 mapping and monitoring, *Aeolian Research*, 23, 63–78,
441 <https://doi.org/10.1016/j.aeolia.2016.09.006>, 2016.
- 442 8. China Meteorology Administration (CMA): National basic meteorological station
443 in Guangzhou was relocated four times in 62 years:

- 444 http://www.cma.gov.cn/2011xwzx/2011xmtjj/201110/t20111026_121807.html,
445 last access: 22 December 2023, 2011.
- 446 9. China Meteorology Administration (CMA): Notice of the China meteorological
447 administration on the issuance of provisional regulations on relocation and
448 removal of national ground meteorological observation stations:
449 http://www.gov.cn/gongbao/content/2013/content_2344560.htm, last access: 22
450 December 2023, 2012.
- 451 10. China Meteorological Administration (CMA): Meteorological data set description
452 document:
453 http://101.200.76.197:91/mekb/?r=data/detail&dataCode=SURF_CLI_CHN_MU
454 [L_DAY_V3.0](http://101.200.76.197:91/mekb/?r=data/detail&dataCode=SURF_CLI_CHN_MU), last access: 22 December 2023, 2017.
- 455 11. Dunn, R. J. H., Azorin-Molina, C., Menne, M. J., Zeng, Z., Casey, N. W., and
456 Shen, C.: Reduction in reversal of global stilling arising from correction to
457 encoding of calm periods, *Environ. Res. Commun.*, 4, 061003,
458 <https://doi.org/10.1088/2515-7620/ac770a>, 2022.
- 459 12. Feng, S., Hu, Q., and Qian, W.: Quality control of daily meteorological data in
460 China, 1951–2000: a new dataset, *International Journal of Climatology*, 24, 853–
461 870, <https://doi.org/10.1002/joc.1047>, 2004.
- 462 13. Fu, G., Yu, J., Zhang, Y., Hu, S., Ouyang, R., and Liu, W.: Temporal variation of
463 wind speed in China for 1961–2007, *Theoretical and Applied Climatology*, 104,
464 313–324, <https://doi.org/10.1007/s00704-010-0348-x>, 2011.
- 465 14. He, Y., Chan, P. W., and Li, Q.: Standardization of raw wind speed data under
466 complex terrain conditions: A data-driven scheme, *Journal of Wind Engineering*
467 *and Industrial Aerodynamics*, 131, 12–30,
468 <https://doi.org/10.1016/j.jweia.2014.05.002>, 2014.
- 469 15. Hong, H. P., Mara, T. G., Morris, R., Li, S. H., and Ye, W.: Basis for
470 recommending an update of wind velocity pressures in Canadian design codes,
471 *Can. J. Civ. Eng.*, 41, 206–221, <https://doi.org/10.1139/cjce-2013-0287>, 2014.
- 472 16. Hu, W., Kong, L., Zhu, X., & Xue, W.: Accuracy analysis on contact
473 anemometer self – recording records digitization processing system, *Journal of*

- 474 Arid Meteorology, 27, 168-171, <http://www.ghqx.org.cn/CN/Y2009/V27/I2/168>,
475 2009. [In Chinese]
- 476 17. Killick, R., Fearnhead, P., and Eckley, I. A.: Optimal Detection of Changepoints
477 With a Linear Computational Cost, Journal of the American Statistical
478 Association, 107, 1590–1598, <https://doi.org/10.1080/01621459.2012.737745>,
479 2012.
- 480 18. Li, Y., Chen, Y., Li, Z., and Fang, G.: Recent recovery of surface wind speed in
481 northwest China, International Journal of Climatology, 38, 4445–4458,
482 <https://doi.org/10.1002/joc.5679>, 2018.
- 483 19. Liu, F., Sun, F., Liu, W., Wang, T., Wang, H., Wang, X., and Lim, W. H.: On
484 wind speed pattern and energy potential in China, Applied Energy, 236, 867–876,
485 <https://doi.org/10.1016/j.apenergy.2018.12.056>, 2019.
- 486 20. Liu, Y., Zeng, Z., Xu, R., Ziegler, A. D., Jerez, S., Chen, D., Azorin-Molina, C.,
487 Zhou, L., Yang, X., Xu, H., Li, L., Dong, L., Zhou, F., Cao, R., Liu, J., Ye, B.,
488 Kuang, X., and Yang, X.: Increases in China’s wind energy production from the
489 recovery of wind speed since 2012, Environ. Res. Lett., 17, 114035,
490 <https://doi.org/10.1088/1748-9326/ac9cf4>, 2022.
- 491 21. Liu, Y., Xu, R., Ziegler, A. D., and Zeng, Z.: Stronger winds increase the sand-
492 dust storm risk in northern China, Environ. Sci.: Atmos., 2, 1259–1262,
493 <https://doi.org/10.1039/D2EA00058J>, 2022.
- 494 22. Masters, F. J., Vickery, P. J., Bacon, P., and Rappaport, E. N.: Toward Objective,
495 Standardized Intensity Estimates from Surface Wind Speed Observations,
496 Bulletin of the American Meteorological Society, 91, 1665–1682,
497 <https://doi.org/10.1175/2010BAMS2942.1>, 2010.
- 498 23. McVicar, T. R., Roderick, M. L., Donohue, R. J., Li, L. T., Van Niel, T. G.,
499 Thomas, A., Grieser, J., Jhajharia, D., Himri, Y., Mahowald, N. M.,
500 Mescherskaya, A. V., Kruger, A. C., Rehman, S., and Dinpashoh, Y.: Global
501 review and synthesis of trends in observed terrestrial near-surface wind speeds:
502 Implications for evaporation, Journal of Hydrology, 416–417, 182–205,
503 <https://doi.org/10.1016/j.jhydrol.2011.10.024>, 2012.

- 504 24. Rayner, D. P.: Wind Run Changes: The Dominant Factor Affecting Pan
505 Evaporation Trends in Australia, *Journal of Climate*, 20, 3379–3394,
506 <https://doi.org/10.1175/JCLI4181.1>, 2007.
- 507 25. Shen, C., Zha, J., Wu, J., and Zhao, D.: Centennial-Scale Variability of Terrestrial
508 Near-Surface Wind Speed over China from Reanalysis, *Journal of Climate*, 34,
509 5829–5846, <https://doi.org/10.1175/JCLI-D-20-0436.1>, 2021.
- 510 26. Sohu: Due to lack of sufficient attention, 60% of the national ground
511 meteorological observation stations were forced to relocate,
512 <https://news.sohu.com/20040921/n222160625.shtml>, last access: 22 December
513 2023, 2004. [In Chinese]
- 514 27. Thiessen, A. H.: Precipitation Averages for Large Areas, *Monthly Weather*
515 *Review*, 39, 1082, Thiessen, A. H.: Precipitation Averages for Large Areas,
516 *Monthly Weather Review*, 39, 1082, [https://doi.org/10.1175/1520-0493\(1911\)39<1082b:PAFLA>2.0.CO;2](https://doi.org/10.1175/1520-0493(1911)39<1082b:PAFLA>2.0.CO;2), 1911.
- 518 28. Tian, Q., Huang, G., Hu, K., and Niyogi, D.: Observed and global climate model
519 based changes in wind power potential over the Northern Hemisphere during
520 1979–2016, *Energy*, 167, 1224–1235,
521 <https://doi.org/10.1016/j.energy.2018.11.027>, 2019.
- 522 29. Trewin, B.: Exposure, instrumentation, and observing practice effects on land
523 temperature measurements, *WIREs Climate Change*, 1, 490–506,
524 <https://doi.org/10.1002/wcc.46>, 2010.
- 525 30. Vautard, R., Cattiaux, J., Yiou, P., Thépaut, J.-N., and Ciais, P.: Northern
526 Hemisphere atmospheric stilling partly attributed to an increase in surface
527 roughness, *Nature Geosci*, 3, 756–761, <https://doi.org/10.1038/ngeo979>, 2010.
- 528 31. Wan, H., Wang, X. L., and Swail, V. R.: Homogenization and Trend Analysis of
529 Canadian Near-Surface Wind Speeds, *Journal of Climate*, 23, 1209–1225,
530 <https://doi.org/10.1175/2009JCLI3200.1>, 2010.
- 531 32. Wang, X., Piao, S., Ciais, P., Li, J., Friedlingstein, P., Koven, C., and Chen, A.:
532 Spring temperature change and its implication in the change of vegetation growth

- 533 in North America from 1982 to 2006, Proc. Natl. Acad. Sci. U.S.A., 108, 1240–
534 1245, <https://doi.org/10.1073/pnas.1014425108>, 2011.
- 535 33. Wang, X. L.: Accounting for Autocorrelation in Detecting Mean Shifts in
536 Climate Data Series Using the Penalized Maximal t or F Test, Journal of Applied
537 Meteorology and Climatology, 47, 2423–2444,
538 <https://doi.org/10.1175/2008JAMC1741.1>, 2008.
- 539 34. World Meteorological Organization (WMO): WMO guidelines on the calculation
540 of climate normals WMO-No. 1203, [https://public-](https://public-old.wmo.int/en/resources/library/wmo-guidelines-calculation-of-climate-normals)
541 [old.wmo.int/en/resources/library/wmo-guidelines-calculation-of-climate-normals](https://public-old.wmo.int/en/resources/library/wmo-guidelines-calculation-of-climate-normals),
542 last access: 22 December 2023, 2017.
- 543 35. Organization (WMO): Guide to Instruments and Methods of Observation.
544 Volume V – Quality Assurance and Management of Observing Systems. 2018
545 edition., World Meteorological Organization, <https://doi.org/10.25607/OBP-690>,
546 2018.
- 547 36. Organization (WMO): Guidelines on Homogenization. 2020 edition., World
548 Meteorological Organization, <https://doi.org/10.25607/OBP-1920>, 2020.
- 549 37. Xin, Y., Chen, H., & Li, Y.: Homogeneity adjustment of annual mean wind speed
550 and elementary calculation of fundamental wind pressure over Xinjiang
551 meteorological stations. Climatic and Environmental Research, 17(2), 184-196,
552 [10.3878/j.issn.1006-9585.2011.10093](https://doi.org/10.3878/j.issn.1006-9585.2011.10093), 2012. [In Chinese]
- 553 38. Yang, Q., Li, M., Zu, Z., and Ma, Z.: Has the stilling of the surface wind speed
554 ended in China?, Sci. China Earth Sci., 64, 1036–1049,
555 <https://doi.org/10.1007/s11430-020-9738-4>, 2021.
- 556 39. Zeng, Z., Ziegler, A., Searchinger, T., Yang, L., Chen, A., Ju, K., Piao, S., Li, L.,
557 Ciais, P., Chen, D., Liu, J., Azorin-Molina, C., Chappell, A., Medvigy, D., and
558 Wood, E.: A reversal in global terrestrial stilling and its implications for wind
559 energy production, Nature Climate Change, 9, 1–7,
560 <https://doi.org/10.1038/s41558-019-0622-6>, 2019.

- 561 40. Zha, J., Shen, C., Zhao, D., Wu, J., and Fan, W.: Slowdown and reversal of
562 terrestrial near-surface wind speed and its future changes over eastern China,
563 Environ. Res. Lett., 16, 034028, <https://doi.org/10.1088/1748-9326/abe2cd>, 2021.
- 564 41. Zhang, G., Azorin-Molina, C., Wang, X., Chen, D., McVicar, T. R., Guijarro, J.
565 A., Chappell, A., Deng, K., Minola, L., Kong, F., Wang, S., and Shi, P.: Rapid
566 urbanization induced daily maximum wind speed decline in metropolitan areas: A
567 case study in the Yangtze River Delta (China), Urban Climate, 43, 101147,
568 <https://doi.org/10.1016/j.uclim.2022.101147>, 2022.
- 569